IEEE Access
Multidisciplinary | Rapid Review | Open Access Journal

Received March 14, 2020, accepted March 26, 2020, date of publication March 30, 2020, date of current version April 14, 2020.

Digital Object Identifier 10.1109/ACCESS.2020.2984363

A Miniaturized Wideband Dual-Polarized Antenna Based on Mode-Control Principle for Base-Station Applications

DONGZE ZHENG[1], (Student Member, IEEE), YU LUO[2], (Member, IEEE), AND QING-XIN CHU[3], (Fellow, IEEE)

[1]Department of Electrical Engineering, Poly-Grames Research Center, Polytechnique Montreal, Montreal, QC H3T 1J4, Canada
[2]Tianjin Key Laboratory of Imaging and Sensing Microelectronics Technology, School of Microelectronics, Tianjin University, Tianjin 300072, China
[3]School of Electronic and Information Engineering, South China University of Technology, Guangzhou 510640, China

Corresponding author: Yu Luo (yluo@tju.edu.cn)

This work was supported in part by the Independent Innovation Fund of Tianjin University under Grant 2019XRY-0017.

ABSTRACT In this paper, a miniaturized wideband dual-polarized antenna and its array are proposed and demonstrated for practical base-station applications. "Mode-control" principle is employed to facilitate both miniaturization and bandwidth-enhancement of the proposed antenna element. To be more specific, by inserting meander lines into a traditional crossed loop-dipole antenna, its first resonant mode can be shifted to a lower frequency without increasing the aperture size, implying that a total size reduction can be achieved. Meanwhile, by embedding a pair of crossed straight strips into the coupling region of the crossed loop-dipole antenna, its second resonant mode can be moved to a higher frequency with a good impedance matching, thereby improving the impedance bandwidth significantly. A prototype of the proposed antenna with a small radiator size of only $0.33\lambda \times 0.33\lambda$ (λ is the wavelength at the center frequency of 2.2 GHz) is designed, fabricated and measured. Measurements show that in the target frequency band from 1.71 GHz to 2.69 GHz, i.e., 2G/3G/4G bands, a relatively good impedance matching with the VSWR of less than 1.65 and a high isolation of greater than 28 dB are obtained by the proposed antenna element. Also, a stable gain of 8.7 ± 0.5 dBi and a stable 3-dB beamwidth of $64.8\pm2.7°$ at the H-plane are respectively achieved. A multiple-input-multiple-output (MIMO) antenna array consisting of two subarrays with electrical down-tilt is further developed for practical base-station applications. Each subarray is composed of ten antenna elements. The overall width of the array is only 260 mm, which is much narrower than that of typical industrial products ($\sim$305 mm). Measured results show that the antenna array has also achieved good performances such as wide impedance bandwidth, high isolations among different ports, and stable radiations over the 2G/3G/4G bands.

INDEX TERMS Antenna array, base-station, dual-polarized, electrical down-tilt, miniaturized, mode-control, multi-array, multimode, multiple-input-multiple-output (MIMO), wideband, 2G/3G/4G.

I. INTRODUCTION

With the rapid development of wireless communication systems, more and more communication standards (e.g., 2G, 3G, and 4G) are coexistent over the long term and thus should be incorporated and co-designed into the same base-station to save its installation space and costs of operation and maintenance. To this end, multi-array multi-/wide-band antennas simultaneously supporting several frequency bands and standards (DCS/PCS/UMTS/LET, for example) are attractive and thus have received much attention in recent years. Particularly, in order to save the whole space of the base-station antenna, two or more antenna arrays are arranged closely and share the same antenna reflector and radome [1]. However, this will bring the difficulty to ensure the performances of each array satisfactory, since the mutual coupling or cross-band interference among these closely arranged arrays is significant. As a whole, there are mainly two challenges needed to be tackled in the design of multi-array multi-/wide-band base-station antennas. Firstly, in order to simplify the design process of an antenna array, it is preferable to adopt the same antenna element covering several frequency bands simultaneously; thus, the base-station antenna element with a wide impedance bandwidth to cover more

The associate editor coordinating the review of this manuscript and approving it for publication was Davide Comite.

This work is licensed under a Creative Commons Attribution 4.0 License. For more information, see https://creativecommons.org/licenses/by/4.0/

frequency bands is naturally needed. Secondly, for the antenna element, it should have a small aperture size or occupied area so that the size of the whole antenna array can be reduced. This is critical since the space in a base-station tower is very limited, not to mention that some room should be reserved for the emerging 5G antennas which should be treated separately due to their different system configurations compared to that of the current 2G/3G/4G systems. Also note that the mutual coupling between array elements or subarrays can be suppressed to some extent if the antenna element has a compact size. On the other hand, diversity techniques, which are mainly in the forms of polarization diversity (dual polarization, for example) and space diversity, have been widely deployed in base-stations since decades, acting as an effective method to improve the channel capacity and data rate, reduce multi-patch fading, and increase spectral efficiency, etc [2]. As a consequence, miniaturized wideband dual-polarized antennas and arrays have been in the spotlight of current base-station antennas and receiving much attention by researchers and engineers.

In recent years, significant developments in the design of wideband dual-polarized antennas on the basis of various antenna types have been presented to meet practical applications, such as patch antennas [3]–[5], slot antennas [6]–[8], magneto-electric dipoles [9]–[11], folded or curved dipoles [12]–[16], and tightly-coupled crossed-dipole antennas [17]–[25]. Specifically, for those patch antennas [3]–[5], several good performances, i.e., high isolation and low cross-polarization can be easily obtained by adopting special feeding mechanisms. However, they suffer from complicated structures and insufficient bandwidth (15%, 20%, and 22.2% respectively) for 2G/3G/4G applications. Although the dual-polarized slot antennas proposed in [6], [7] have wide impedance bandwidth (45.8% and 38.7% respectively) and high isolation (greater than 33 dB and 35 dB, respectively), they all have large aperture sizes ($1.1\lambda_0 \times 1.1\lambda_0$ and $0.51\lambda_0 \times 0.51\lambda_0$ respectively) due to the natural property of slot antennas. Dual-polarized antennas based on magneto-electric dipoles were proposed in [9]–[11] with wide impedance bandwidth, stable radiation, stable gain and low cross-polarization. However, they all suffer from drawbacks of bulky structures and large radiators ($0.51\lambda_0 \times 0.51\lambda_0$, $0.62\lambda_0 \times 0.62\lambda_0$, and $0.47\lambda_0 \times 0.47\lambda_0$, respectively). A series of wideband dual-polarized antennas [12]–[30] based on folded/curved/crossed dipoles with various configurations and shapes are good candidates to be potentially applied to base-stations. Nevertheless, some of them are subject to relatively large sizes, insufficient bandwidth, or fabrication difficulty, which make them relatively unsatisfactory to be adapted to current base-station applications and developments.

On the other hand, although several works regarding dual-polarized multi-/wide-band antenna arrays have been reported to meet market demands of base-stations [1], [12], [18], [24]–[31], it is practical to develop a wideband array consisting of several parallel-arranged subarrays operating with polarization diversity and multiple-input-multiple-output (MIMO) techniques to satisfy the ever-increasing demands of communication services. In this sense, however, the occupied area of the whole array will be the main bottleneck in the network construction (e.g., the base-station tower); this makes the design of miniaturized wideband antenna elements with satisfactory performances critical, promising and urgent. Unfortunately, it is a well-known dilemma for antennas to possess both the wide bandwidth and miniaturized size simultaneously (normally, a compromise should be made between the two behaviors), although such antennas are stringently required by base-station industry. This issue will be more severe when practical situations such as fabrication difficulty and cost, structural strength, and mass-production are considered. In this paper, a miniaturized wideband dual-polarized antenna element and its array are proposed and developed for base-station applications. Printed crossed square-loop-dipole antenna, which is a popular candidate featuring simple configuration, easy fabrication, and low cost, is selected as the initial template. ''Mode-control'' principle is then employed for it with the help of meandering lines and coupled straight strips. Because of this, the original two resonant modes of the traditional crossed loop-dipole antenna can be flexibly tailored, paving the way to simultaneously realize miniaturization and bandwidth-enhancement to some extent. Based on the miniaturized wideband antenna element, a small-sized MIMO antenna array composed of two subarrays is developed for practical 2G/3G/4G base-station applications. Both the antenna element and the array have achieved good performances, such as wide impedance bandwidth, high isolation, high gain and stable radiation patterns over the target frequency band.

II. MINIATURIZED WIDEBAND DUAL-POLARIZED ANTENNA ELEMENT

A. ANTENNA STRUCTURE

The geometry of the proposed miniaturized wideband dual-polarized antenna element is illustrated in Figure 1. In order to have a good description about the antenna element, we define *xoz*-plane as the horizontal plane (*H*-plane) and *yoz*-plane as the vertical plane (*V*-plane). Basically, the antenna element is comprised of a pair of crossed loop-dipoles inserted with meander strips, a pair of crossed straight strips that are symmetrically embedded into the coupling gap of crossed loop-dipoles, two T-shaped feeding structures and a box-shaped reflector. All of these loop-dipoles and straight strips are printed on the bottom layer of a low-cost FR4 substrate with a dielectric constant of $\varepsilon_r = 4.4$, a loss tangent of 0.02, and a thickness of $H_d = 0.8$mm. Meanwhile, the two T-shaped feeding structures are printed on the top layer of the substrate. It is noted that to avoid intersection between the two feeding structures, one of them is modified and its partial feeding line is printed on the bottom of the substrate. Therefore, two holes are drilled in the substrate, and two shorting pins are used for connecting the upper part with the bottom part with

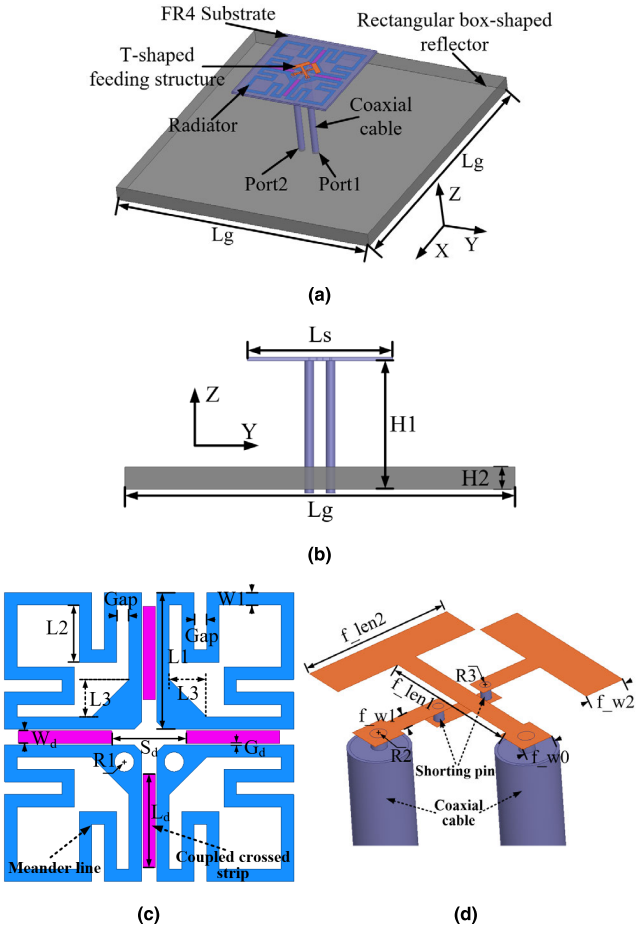

FIGURE 1. Geometry of the proposed antenna element (not to scale). (a) 3D view; (b) side view; (c) top view of the radiator; (d) feeding structure.

respect to this feeding structure. Each loop-dipole is fed by a coaxial cable, whose outer conductor is connected to one arm of the loop-dipole while the inner one is protruded through the substrate and connected to a bonding pad of the T-shaped feeding structure. To have a unidirectional radiation, a square box-shaped reflector is used and located under the substrate with a distance of $H1 = 35$ mm (about 0.25 λ, where λ is the free-space wavelength at 2.2 GHz).

B. WORKING PRINCIPLE

In practical dual-polarized base-station antenna products over the 2G/3G era, the crossed square-loop dipole antennas are popular and promising thanks to its many merits such as simple configuration, easy feeding, high structural strength, low weight, and particularly wide impedance bandwidth. However, its bandwidth and size performances are hardly adapted to and should be improved for the current 2G/3G/4G base-station requirements, as will be demonstrated later. Consequently, when the proposed antenna element was designed, a traditional square loop-dipole was considered initially, with seeking extra bandwidth-enhancement and miniaturization techniques. Figure 2 depicts the evolution of the proposed antenna. Compared to the single-polarized

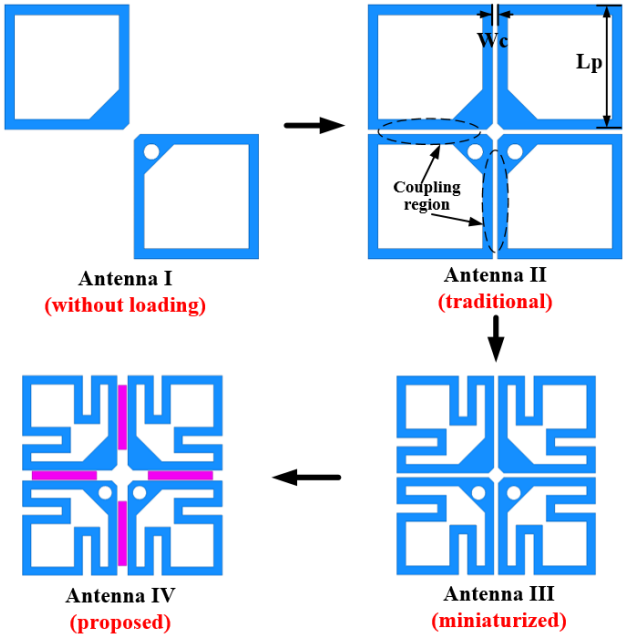

FIGURE 2. Evolution of the proposed antenna element.

square-loop-dipole shown as Ant. I, the traditional dual-polarized version that has two identical crossed loop-dipoles is depicted as Ant. II. When a loop-dipole is driven, the other one is coupled as a parasitic element or resonator due to strong coupling, and the wide impedance bandwidth that are due to multiple resonances can be thus obtained [17]. To make the paper self-contained, provide a background, and also give a clear illustration of how these resonant modes are created and controlled, Figure 3 depicts the dimensional effects of the parasitic polarization element on resonant mode behaviors of the driven loop-dipole. It can be seen obviously that when there is no parasitic polarization element (i.e., $L_r = 0$), only one resonant mode is existent, which corresponds to the well-known half-wavelength (fundamental) resonant mode of a dipole. The introduction of the parasitic polarization element is able to introduce another resonant mode that is located at a higher frequency and can be controlled by changing the side length of the parasitic element. This phenomenon is also included and

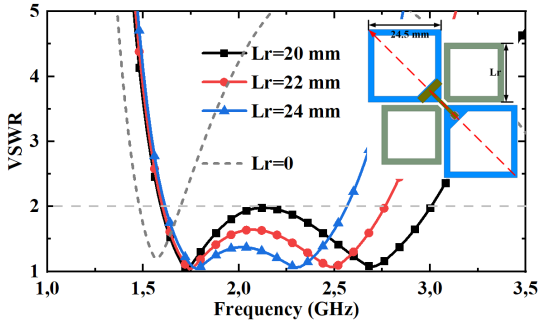

FIGURE 3. Effects of the parasitic loop-dipole on resonant mode behaviors. *Lr* represents the side-length of the parasitic loop-dipole, while the driven one is with a side-length of 24.5 mm, as shown in the inset.

explained in [32] that the driven dipole's bandwidth can be largely extended since its higher-order resonant modes can be shifted to a lower frequency and then combine with the lower-order mode by using and adjusting the parasitic polarization element. In general, the first mode is primarily determined by the current path along the driven loop-dipole, while the second one can be adjusted through the coupling region between crossed loop-dipoles. However, due to the structural limitation that the two polarization elements must be kept identical, the two modes, therefore, cannot be flexibly engineered to obtain a wide impedance bandwidth to cover 2G/3G/4G bands. This is illustrated in Figure 4, which displays that the two resonant modes will be simultaneously influenced when either altering the length of the loop-dipole L_p or the coupling gap width W_c, together with an insufficient impedance bandwidth exhibited. Notably, it is easy to find that L_p is the predominant measure for adjusting and allocating the frequencies of resonant modes while W_c is primarily responsible for impedance matching of the whole antenna. Also note that such two parameters, basically, are the only measures left for Ant. II for mode-control. This will not only bring down the design degrees of freedom, but also result in the insufficient impedance bandwidth for 2G/3G/4G bands as mentioned above and will also be shown later. To solve this predicament, various shapes and configurations of crossed dipoles that shares the same impedance-enhancement principle have been proposed in [18]–[30], and basically most of them can be interpreted with the concern of how to flexibly control and allocate the frequency locations of relevant resonant modes, i.e., mode-control, to realize wide impedance bandwidth. For example,

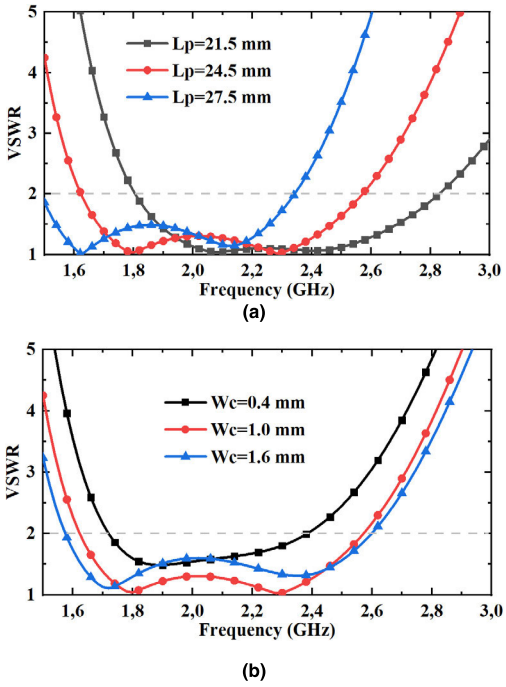

FIGURE 4. An illustration of the incapability of flexible mode-control for the traditional crossed loop-dipole antenna in terms of the effects of (a) side-length *Lp* and (b) coupling gap width *Wc* on the VSWR.

the work in [21] uses the octagonal loop-dipole whereby the current path of the driven dipole can be increased without influencing the coupling region's dimensions (i.e., length). Because of this, its first resonant mode can be independently shifted to a lower frequency without influencing the second mode, and thus the wide impedance bandwidth can be eventually realized. Interestingly, the work in [18] that makes use of bow-tie dipoles also share such specific mode-control behaviors and mechanisms as [21]. The crossed chamfered loop-dipole antenna in [23], [29], contrastively, is able to provide a second mode that can be independently controlled to a higher frequency so as to enhance the impedance bandwidth. This is because only the length of the coupling region is shortened without influencing the driven dipole's current path when resizing the chamfer. It is concluded from the above analysis that for such a class of crossed dipole antennas, if an independently controllable first mode is required, the current path of the driven dipole should be altered but remaining the dimensions of the coupling region unchanged, just like the works [18], [21] do. Meanwhile, if an independently controllable second mode is needed, the coupling region dimensions should be modified while the current path of the driven dipole should be kept constant, which is similar as [23], [29].

The authors proposed an approach to widen the impedance bandwidth of the original crossed loop-dipole antenna (i.e., Ant. II), which is based on embedding extra small loops into it [22]. This can introduce an additional and flexibly controllable third resonant mode for impedance bandwidth enhancement but without increasing the radiator size of the antenna. Another method proposed by the authors is based on the mode-control principle with resort to stepped loop-dipoles and embedded straight strips [24]. Unfortunately, although independently controllable resonant modes and wide impedance bandwidth can be realized, enlarged radiator size caused by the arms of the stepped loop-dipole is unavoidable. Here, based on the embedding scheme in [22] and the mode-control principle in [24], an idea of bandwidth-enhancement while realizing radiator-miniaturization for a crossed loop-dipole antenna is established: the first resonant mode can be moved to a lower frequency by an inserted structure inside the loop-dipole like [22] while the second mode is adjusted by the coupled straight strips similar to [24]. To facilitate this miniaturization and bandwidth-enhancement concept, two techniques are employed. First, instead of adopting a regular square-loop-dipole, meander lines are inserted into the loop-dipole, i.e., the Ant. III, as shown in Figure 2. By doing so the first resonant mode can be shifted to a lower frequency thanks to the lengthened current path but without increasing the occupied area, and this will be confirmed later. In other words, to a given frequency of resonant mode, a miniaturized structure can be formed. On the other hand, crossed straight strips are embedded into the coupling gap of the crossed miniaturized loop-dipoles, and the whole structure is depicted as the Ant. IV (the proposed one) in Figure 2. Its upper resonant mode can be independently controlled by altering

the length and position of these embedded straight strips. Consequently, it can be moved toward a higher frequency for an enhanced impedance bandwidth with good impedance matching simultaneously achieved. Dimensional effects of the inserted meander line and embedded coupling strips on resonant modes can be seen in Figure 5(a) and (b) respectively, illustrating that both the first and second modes can be independently controlled by adjusting $L2$ and L_d, respectively. Note that the distance of straight stripes S_d can also be used for exclusively adjusting the second mode, which is not plotted here for brevity. Figure 6 depicts a comparison of several antennas in Figure 2 in terms of their VSWR and gain performances. It can be seen obviously that Ant. II and III have the same first resonant mode of 1.8 GHz, implying that the current paths along the driven loop-dipole in the two are the same. However, the radiator size of Ant. III is obviously smaller than that of Ant. II due to the inserted meander lines. The upper resonant mode of Ant. III is slightly higher than that of Ant. II because of the shortened coupling length of crossed dipoles, as expected. Meanwhile, a deteriorated impedance matching is also observed in the vicinity of this resonant mode for the case of Ant. III. It can be found apparently that both Ant. II and III do not have sufficient bandwidth for 2G/3G/4G bands. In order to move the upper resonant mode to a higher frequency for bandwidth-enhancement and to improve the impedance matching situation, a pair of crossed straight strips are embedded into Ant. III; thus Ant. IV, the proposed one, is formed. Compared to Ant. III possessing a miniaturized size but limited bandwidth, the proposed Ant. IV has a wider impedance bandwidth and improved matching condition, with a miniaturized size preserved. Also note that when talking about the gain performances of these antennas in Figure 2, although the meander lines are used in the proposed antenna, it does not suffer from obvious gain loss but own the benefits of miniaturized size and improved bandwidth compared to its original counterpart. It is necessary to mention that the embedded straight strips just work an effective approach to adjust the coupling effects of crossed loop-dipoles; these strips do not contribute to the radiation in the far-field since the currents distributed on the them form a narrow-loop-shape exhibiting oppositely directed currents, as can be seen from Figure 7 illustrating the current distribution of the proposed antenna at 2.2 GHz.

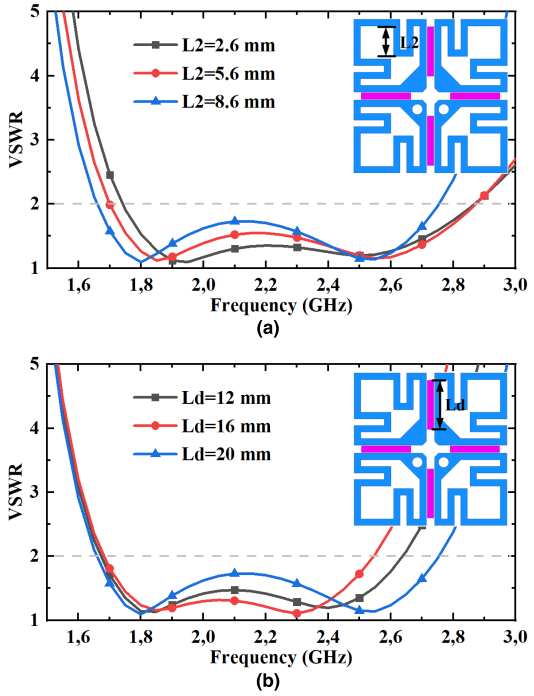

FIGURE 5. An illustration of the capability of flexible mode-control for the proposed antenna in terms of the effects of (a) meander line length $L2$ and (b) coupling strip length Ldi on the VSWR.

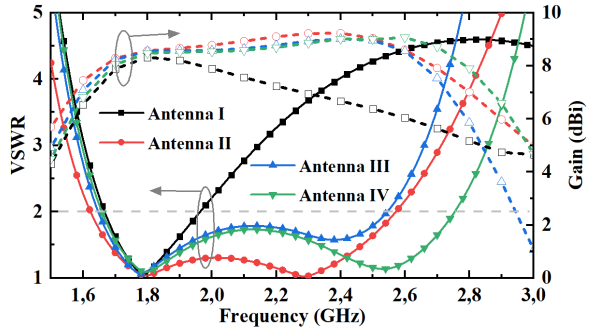

FIGURE 6. A comparison of several antennas with respect to the VSWR and gain performances. These antennas can be found in Figure 2.

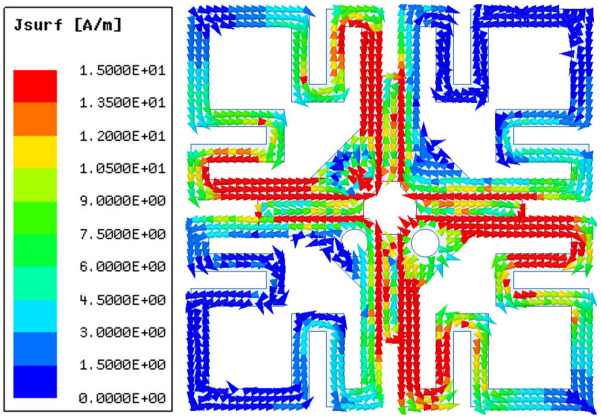

FIGURE 7. Current distributions at 2.2 GHz when port 1 is excited. Current distributions at other frequencies are similar to this and thus are not given here for brevity.

C. SIMULATED AND MEASURED RESULTS

To verify the design, a prototype of the proposed antenna element with finally optimized parameters listed in Table 1 was fabricated and measured. The photograph of the fabricated antenna is shown in Figure 8. Measured results in terms of VSWRs, gains, and radiation patterns were respectively obtained by an Agilent N5230A network analyzer and a far-field measurement system. Figure 9 shows the simulated and measured VSWR and port-to-port isolation of the proposed antenna element. It can be found that the measured overlapped impedance bandwidth of the two ports is 48.2% with VSWR $<$ 2 from 1.68 to 2.74 GHz (the VSWR is less

TABLE 1. Dimensions of the proposed antenna elementi.

Parameter	L_g	L_S	*H1*	*H2*	H_d	*L1*
Value (mm)	145	54	35	6	0.8	21.4
Parameter	*L2*	*L3*	*Gap*	*W1*	W_d	L_d
Value (mm)	9.2	6	2	2	2	12
Parameter	S_d	G_d	*R1*	*R2*	*R3*	*f_w0*
Value (mm)	6	0.2	1.58	0.46	0.3	2
Parameter	*f_w1*	*f_len1*	*f_w2*	*f_len2*		
Value (mm)	1	9.8	2.5	9.3		

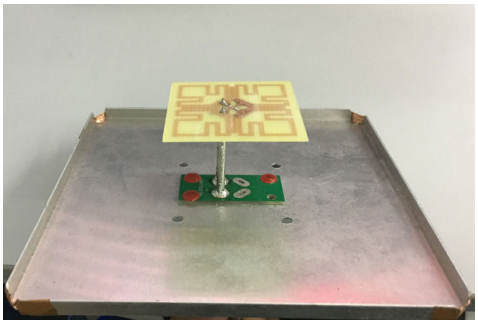

FIGURE 8. Fabricated prototype of the proposed antenna element.

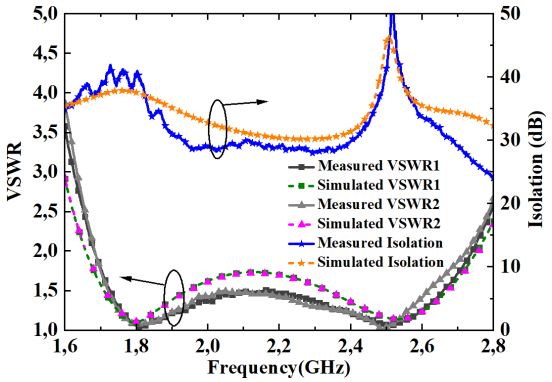

FIGURE 9. Simulated and measured VSWR and isolation of the proposed antenna element.

than 1.65 from 1.71 GHz to 2.69 GHz for 2G/3G/4G bands), which is slightly narrower but shows an mildly improved matching compared to the simulated counterpart. Fabrication errors that results in mode-shifting should be responsible for this. A further improvement of the impedance matching for the proposed antenna can be potentially realized by using delicately designed feeding mechanisms, such as the Y-/L-shaped feeding structures in [12], [21], [23], [29], or the microstrip feeding networks in [14], [16], [19], [20]. The measured isolation between the two ports is greater than 28 dB, agreeing well with the simulated result. Figure 10 depicts the simulated and measured 3-dB beamwidths (H-plane) and gains as a function of frequency from 1.7 GHz to 2.7 GHz when port1 is excited, showing that the measured gain is 8.7 ± 0.5 dBi while the corresponding simulated counterpart is 8.3 ± 0.9 dBi. Also, the measured 3-dB beamwidth is 64.8° ± 2.7° at the H-plane, while the

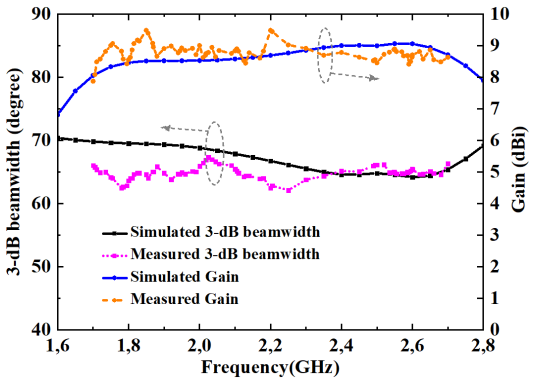

FIGURE 10. Simulated and measured H-plane 3-dB beamwidth and gain of the proposed antenna element when port 1 is excited.

simulated one is 66° ± 3.8°. It can be seen that the measured results are in a relatively good agreement with the simulated ones. Simulated and measured radiation patterns in the H-plane and V-plane at different frequencies of 1.7 GHz, 2.2 GHz and 2.7 GHz are respectively plotted in Figure 11,

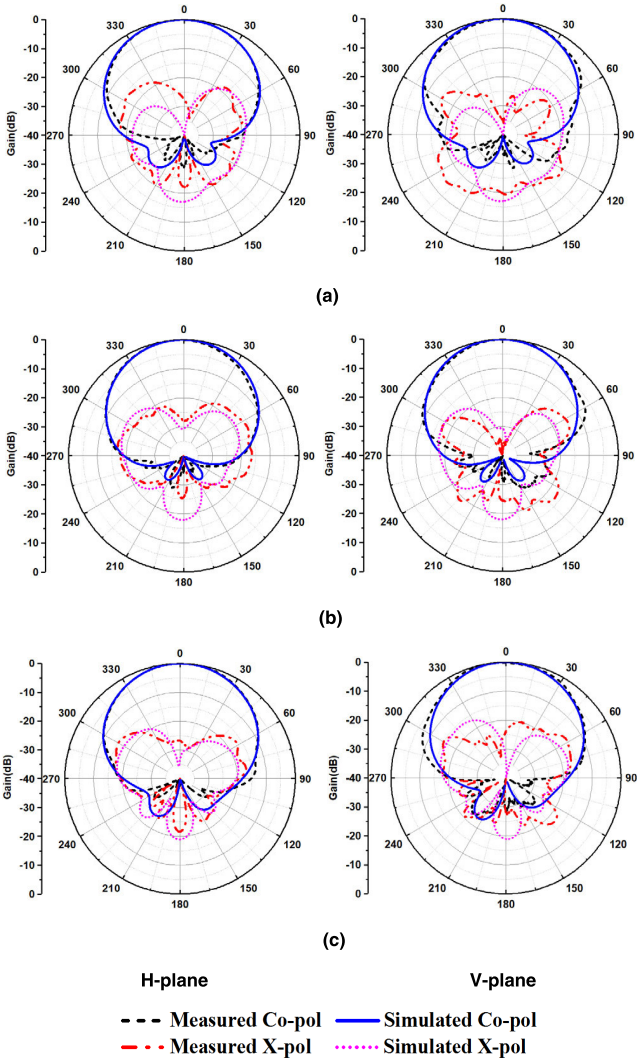

FIGURE 11. Simulated and measured radiation patterns of port1 in terms of *H*-plane and *V*-plane. (a) 1.7 GHz; (b) 2.2 GHz; (c) 2.7 GHz.

TABLE 2. Comparison of several antenna elements developed for 2G/3G/4G bands.

Ref.	Bandwidth (GHz)	Radiator size (mm^2)	Isolation (dB)	Gain (dBi)	HPBW (degree)	XPD (0^O)	XPD ($\pm 60^O$)
[14]	1.69-2.71	70.4×70.4	28	9.8±0.9	66.5°±5.5°	25 dB	N/A
[15]	1.71-2.69	80×80	30	9.3	64°±1°	25 dB	10 dB
[16]	1.69-2.72	46.7×46.7	35	8.6±0.9	68.7°±2.5°	19 dB	10 dB
[18]	1.7-2.7	56×56	30	8.5	65°±8°	20 dB	N/A
[19]	1.7-2.9	66.5×66.5	35	7.8±0.8	N/A	18 dB	N/A
[20]	1.68-2.74	61×61	22	8.2	61.8°±4°	19 dB	N/A
[21]	1.7-2.7	53.5×53.5	25	8.2±0.6	68°±2°	N/A	N/A
[22]	1.68-2.83	52.5×52.5	27	8.8±0.7	65.4°±2.4°	N/A	N/A
[24]	1.68-2.94	50.5×50.5	28.5	8.5±0.9	66.2°±3.7°	N/A	N/A
[25]	1.43-2.9	75.4×75.4	20	8	65°±11°	21.7 dB	N/A
[27]	1.7-2.7	53×53	30	8.5±0.4	65.2°±5.6°	N/A	N/A
This work	1.71-2.69	**45.2×45.2**	28	8.7±0.5	64.8°±2.7°	26 dB	7 dB

illustrating that the antenna element has a stable radiation pattern with low cross-polarization level across the entire target frequency band. The measured radiation patterns agree well with the simulated counterparts. A comparison between the proposed antenna and several antennas in references is tabulated in Table 2 to highlight the benefits of the proposed work. Notably, all the antennas in this table are developed for 2G/3G/4G bands. Dimensional comparison in terms of antenna element's reflector is not considered here as the array developments equipped with large reflectors must be deployed for practical base-station applications, in which the antenna radiator's dimension is critical and will be the bottleneck for reducing the whole size of the array. It can be observed obviously that the proposed antenna is relatively superior, exhibiting the smallest aperture size, sufficient impedance bandwidth for 2G/3G/4G bands, relatively high isolation, moderate gain, acceptable XPD behaviors, and stable 3-dB beamwidth. Also note that most of the works in the table are short of independently controllable resonant modes, thereby potentially being subject to some issues such as the design degrees of freedom and post-debugging processes before mass-production in actuality.

III. DUAL-POLARIZED 2 × 10 MIMO ANTENNA ARRAY

In addition to the popular polarization diversity (e.g., ±45° dual-polarization) that is normally used in base-stations to increase channel capability, reduce multipath fading and improve spectral efficiency, the MIMO technique can also be used to further improve such benefits as mentioned above. In this section, a miniaturized wideband dual-polarized MIMO dual-array is developed to serve practical 2G/3G/4G communication systems.

A. GEOMETRY OF ANTENNA ARRAY

The proposed MIMO antenna array is composed of two subarrays and each subarray consists of ten antenna elements, as shown in Figure 12(a). To suppress the mutual coupling effects between subarrays or array elements, two typical decoupling techniques are adopted: (i) baffles are employed between adjacent array elements and subarrays [1], [4]; (ii) a staggered form is arranged for the two subarrays [31], [33]. Notice that the two approaches mentioned above are effective methods for alleviating mutual coupling, which are often adopted by engineers in practical product developments. There are four ports (i.e., port1, port2, port3 and port4) that are used for feeding the antenna array. Among them, port1 (+45° polarization) and port2 (−45° polarization) are subject to the subarray I and the other two ports (i.e., port3 and port4) belong to the subarray II with the same polarization order. Besides these feeding ports, twenty two-way power dividers and four five-way phase shifters are employed together as feeding networks in the array to feed those antenna elements and realize an electrical down-tilt of the radiation beam. For one polarization of each subarray, as shown in Figure 12(b),

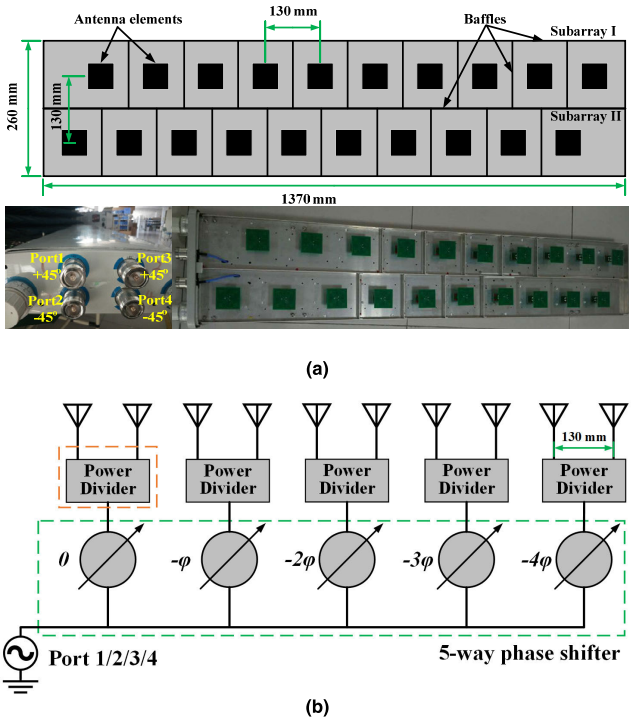

FIGURE 12. (a) Simplified configuration and fabricated prototype of the proposed array. (b) Layout of the array feeding mechanism.

one five-way phase shifter is used with its five outputs connected to five two-way power dividers; each power divider is connected to two adjacent antenna elements sharing the same polarization direction [12], [15]. The spacing between two adjacent antenna elements in a subarray is 130 mm (approximately 0.95 λ at 2.2 GHz), which is selected deliberatively to obtain a high gain with the use of a limited quantity of antenna elements but free from significant appearance of grating lobes. The distance between the two subarrays, which is defined as the distance of the center lines of subarrays, is chosen to be 130 mm as well. Also, lateral baffles (sidewalls) of 20 mm are mainly used for beamwidth-adjusting. Notably, the width of the presented array is only 260 mm, showing a significant size reduction compared with that in commercial products (∼305 mm) [34]. The total size of this array is 1370 × 260 × 35 mm^3.

B. PERFORMANCES OF ANTENNA ARRAY

Figure 13(a) depicts the measured VSWRs and isolations between port1 and port2, which are the two feeding ports of subarray I. It can be seen obviously that in the target frequency band from 1.71 GHz to 2.69 GHz, a good impedance matching with the VSWR of less than 1.5 is achieved for the two ports, while the measured isolation between them is around 30 dB. Compared to the antenna element, the proposed array exhibits an improved impedance matching, which is mainly due to the insertion losses introduced by the feeding network, i.e., power dividers and phase shifters. As for the subarray II, its measured VSWRs and isolations with respect to port3 and port4 are exhibited in Figure 13(b), indicating that satisfactory performances similar as that of the subarray I are also obtained in the target frequency band. Meanwhile, as for the isolations between different ports of different subarrays, namely, the isolations of port 1&3, port 1&4, port 2&3 and port 2&4, Figure 14 indicates that all the port isolation performances are greater than 30 dB within the whole operating bandwidth. Note that all these results shown in Figure 13 and 14 are under the case without electrical down-tilt. The corresponding results with electrical down-tilt from 0° to 10° are also good and thus are not shown here for brevity. Figure 15 displays the measured radiation patterns of the proposed antenna array at different frequencies of 1.7 GHz, 2.2 GHz and 2.7 GHz with different electrical down-tilt degrees. Note that only measured results of port1 are given for brevity and similar results can be observed as well in other ports. It can be seen that for a given degree of down-tilt, the radiation patterns are stable with the change of frequencies in both the *H*-plane and *V*-plane. Meanwhile, for a given frequency, the radiation patterns also remain relatively stable when the electrical down-tilt increases from 0° to 10°. Relatively symmetrical radiation patterns can be observed in the *H*-plane even though the reflector is not symmetrical to each subarray in this plane. The reason for this is that the reflector's dimension is already electrically large compared to the antenna radiator and thus its geometrical asymmetry would not influence significantly on *H*-plane radiation patterns. Although the element spacing is slightly larger than one free-space wavelength at 2.7 GHz in the *V*-plane, grating lobes at this frequency are not significant because of the suppression effects introduced by the element pattern, according to the array's pattern multiplication theorem [35]. However, grating lobes appear to be relatively deteriorated when the down-tilt is 10°, since in this case the suppression effects caused by the element pattern become weak at the current grating lobe directions. For a further improvement of the proposed array in terms of its side/grating lobe behaviors, a tapered illumination and shorter element spacing can be

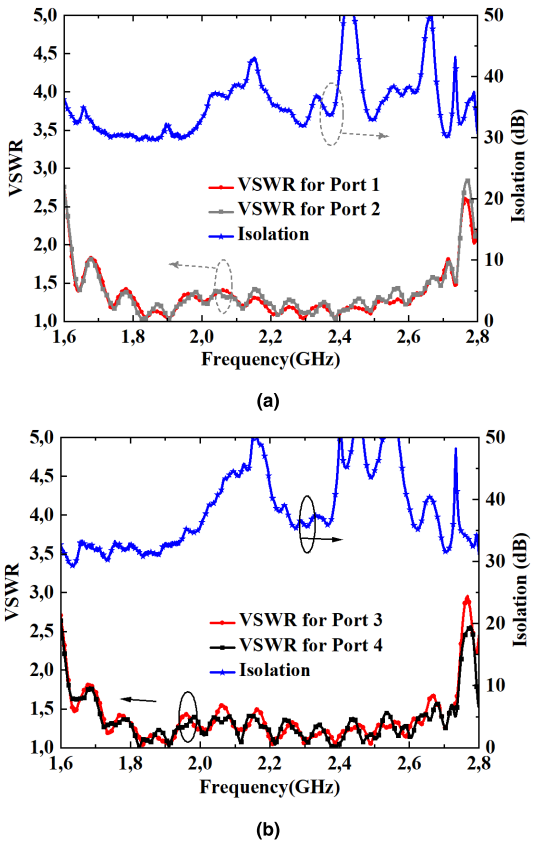

FIGURE 13. Measured VSWR and isolation of different subarrays with respect to (a) port 1 and port 2; (b) port 3 and port 4.

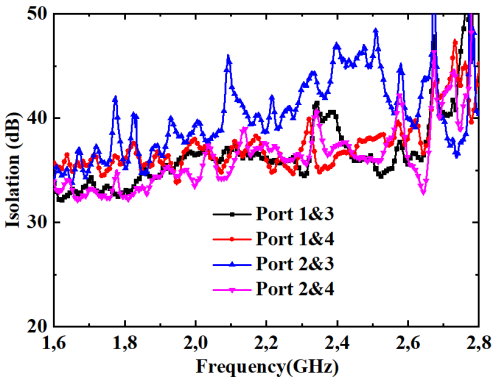

FIGURE 14. Measured isolations among different ports of different subarrays.

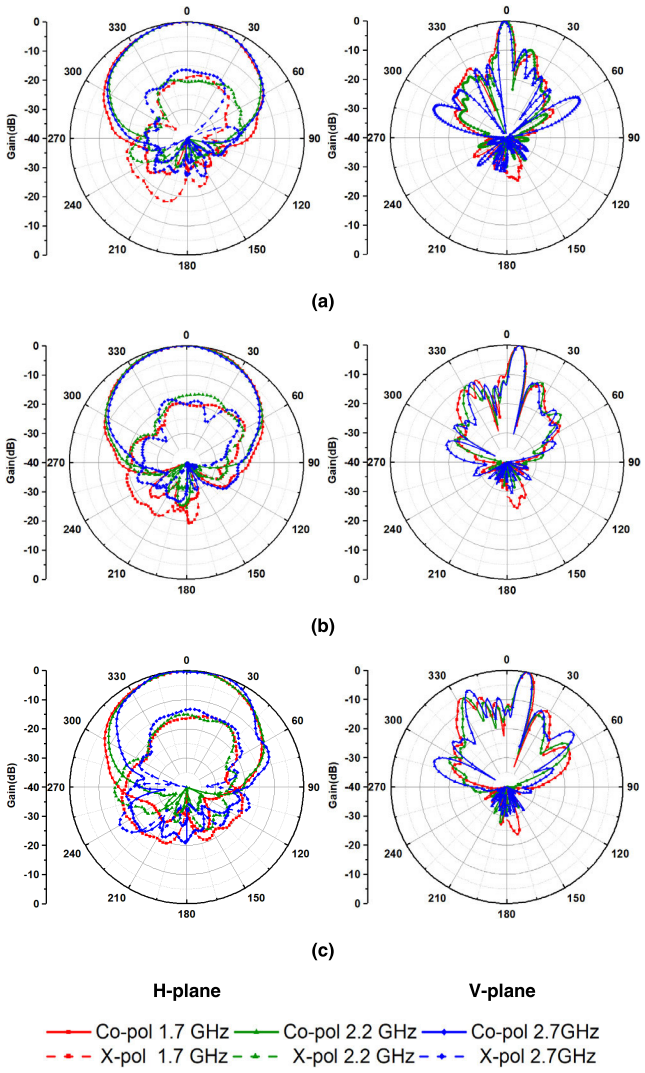

FIGURE 15. Measured radiation patterns of the proposed array with electrical down-tilt of (a) 0°, (b) 5°, and (c) 10°.

TABLE 3. Measured half-power beamwidth at the H-Plane and gain of the antenna array when port 1 is excited.

Frequency (GHz)	No Down Tilt		5° Down Tilt		10° Down Tilt	
	HPBW (degree)	Gain (dBi)	HPBW (degree)	Gain (dBi)	HPBW (degree)	Gain (dBi)
1.7	71.1	14.9	70.2	14.2	69.6	13.8
1.9	67.2	15.2	66.4	14.9	65.2	14.3
2.2	61.9	15.8	62.8	15.2	64	14.9
2.5	60.5	16.3	62.6	15.8	63.9	14.8
2.7	61.2	15.3	63.4	14.9	63.2	14.2

implemented. The measured 3-dB beamwidth in the H-plane and gain of the antenna array with different frequencies and down-tilt degrees are tabulated in Table 3. Over the frequency band from 1.7 GHz to 2.7 GHz, the measured 3-dB beamwidths in the H-plane with 0°, 5° and 10° down-tilt are $65.8 \pm 5.3°$, $65.7 \pm 4.5°$, $66.4 \pm 3.2°$, respectively. Besides, the measured gain of the antenna array with 0° down-tilt is 15.6 ± 0.7 dBi, while the corresponding results for 5° and 10° down-tilt are 15.0 ± 0.8 dBi, 14.5 ± 0.7 dBi, respectively. It can be seen that the gain of this antenna array shows a downward trend with the increase of down-tilt degree. Both the increasing side-lobes and cross-polarization level with the degree of down-tilt should be responsible for this. In general, the proposed antenna array has acceptable electrical performances and miniaturized size, and it can be applied to current base-station applications.

IV. CONCLUSION

A miniaturized wideband dual-polarized antenna element and its array have been proposed and developed for 2G/3G/4G base-station applications. Compared to the traditional loop-dipole antenna that suffers from inflexible mode-control capability and insufficient impedance bandwidth, the proposed antenna element makes use of inserted meander lines and coupled straight strips to flexibly control its resonant modes with achieving reduced radiator size and improved impedance bandwidth. Consequently, a miniaturized radiator size of 45.2 mm × 45.2 mm and wide bandwidth covering from 1.71 GHz to 2.69 GHz are obtained for the proposed antenna element. Also, an antenna array consisting of two subarrays with electrical down-tilt has been developed for practical base-station applications. Both polarization diversity and MIMO techniques are deployed in this array. The width of the presented array is only 260 mm, showing a significant size reduction compared with that in commercial products (∼305 mm). Both the antenna element and array have achieved satisfactory performances, such as small size, wide impedance bandwidth, high isolation, and stable radiation. Own to these desirable features, the proposed antenna will find potential in practical base-station applications.

REFERENCES

[1] Y. He, Z. Pan, X. Cheng, Y. He, J. Qiao, and M. M. Tentzeris, "A novel dual-band, dual-polarized, miniaturized and low-profile base station antenna," *IEEE Trans. Antennas Propag.*, vol. 63, no. 12, pp. 5399–5408, Dec. 2015.
[2] Z.-N. Chen, and K.-M. Luk, *Antennas for Base Stations in Wireless Communications*. New York, NY, USA: McGraw-Hill, 2009.
[3] H. Wong, K. L. Lau, and K. M. Luk, "Design of dual-polarized L-probe patch antenna arrays with high isolation," *IEEE Trans. Antennas Propag.*, vol. 52, no. 1, pp. 45–52, Jan. 2004.
[4] J. Li, S. Yang, Y. Gou, J. Hu, and Z. Nie, "Wideband dual-polarized magnetically coupled patch antenna array with high port isolation," *IEEE Trans. Antennas Propag.*, vol. 64, no. 1, pp. 117–125, Jan. 2016.
[5] Y. Li, Z. Zhao, Z. Tang, and Y. Yin, "Differentially-fed, wideband dual-polarized filtering antenna with novel feeding structure for 5G Sub-6 GHz base station applications," *IEEE Access*, vol. 7, pp. 184718–184725, 2019.
[6] X. Jiang, Z. Zhang, Y. Li, and Z. Feng, "A wideband dual-polarized slot antenna," *IEEE Antennas Wireless Propag. Lett.*, vol. 12, pp. 1010–1013, 2013.
[7] R. Lian, Z. Wang, Y. Yin, J. Wu, and X. Song, "Design of a low-profile dual-polarized stepped slot antenna array for base station," *IEEE Antennas Wireless Propag. Lett.*, vol. 15, pp. 362–365, 2016.
[8] Y. Liu, S. Wang, X. Wang, and Y. Jia, "A differentially fed dual-polarized slot antenna with high isolation and low profile for base station application," *IEEE Antennas Wireless Propag. Lett.*, vol. 18, no. 2, pp. 303–307, Feb. 2019.
[9] B. Qun Wu and K.-M. Luk, "A broadband dual-polarized magneto-electric dipole antenna with simple feeds," *IEEE Antennas Wireless Propag. Lett.*, vol. 8, pp. 60–63, 2009.
[10] Q. Xue, S. W. Liao, and J. H. Xu, "A differentially-driven dual-polarized magneto-electric dipole antenna," *IEEE Trans. Antennas Propag.*, vol. 61, no. 1, pp. 425–430, Jan. 2013.

[11] S.-G. Zhou, Z.-H. Peng, G.-L. Huang, and C.-Y.-D. Sim, "Design of a novel wideband and dual-polarized MagnetoElectric dipole antenna," *IEEE Trans. Antennas Propag.*, vol. 65, no. 5, pp. 2645–2649, May 2017.
[12] D.-L. Wen, D.-Z. Zheng, and Q.-X. Chu, "A dual-polarized planar antenna using four folded dipoles and its array for base stations," *IEEE Trans. Antennas Propag.*, vol. 64, no. 12, pp. 5536–5542, Dec. 2016.
[13] L.-H. Wen, S. Gao, Q. Luo, C.-X. Mao, W. Hu, Y. Yin, Y. Zhou, and Q. Wang, "Compact dual-polarized shared-dipole antennas for base station applications," *IEEE Trans. Antennas Propag.*, vol. 66, no. 12, pp. 6826–6834, Dec. 2018.
[14] H. Sun, C. Ding, B. Jones, and Y. J. Guo, "A wideband base station antenna element with stable radiation pattern and reduced beam squint," *IEEE Access*, vol. 5, pp. 23022–23031, 2017.
[15] W. Chen, H. Lin, H. Ding, Y. Liu, M. Chisala, Z. Shen, H. Zhibin, L. Baihui, and R. Wang, "A low profile broadband dual-polarized base station antenna using folded dipole radiation element," *IEEE Access*, vol. 7, pp. 67679–67685, 2019.
[16] H.-H. Sun, C. Ding, H. Zhu, and Y. J. Guo, "Dual-polarized multi-resonance antennas with broad bandwidths and compact sizes for base station applications," *IEEE Open J. Antennas Propag.*, vol. 1, pp. 11–19, Jan. 2020.
[17] Z. Bao, Z. Nie, and X. Zong, "A novel broadband dual-polarization antenna utilizing strong mutual coupling," *IEEE Trans. Antennas Propag.*, vol. 62, no. 1, pp. 450–454, Jan. 2014.
[18] Y. Cui, R. Li, and H. Fu, "A broadband dual-polarized planar antenna for 2G/3G/LTE base stations," *IEEE Trans. Antennas Propag.*, vol. 62, no. 9, pp. 4836–4840, Sep. 2014.
[19] Y. Gou, S. Yang, J. Li, and Z. Nie, "A compact dual-polarized printed dipole antenna with high isolation for wideband base station applications," *IEEE Trans. Antennas Propag.*, vol. 62, no. 8, pp. 4392–4395, Aug. 2014.
[20] H. Huang, Y. Liu, and S. Gong, "A broadband dual-polarized base station antenna with sturdy construction," *IEEE Antennas Wireless Propag. Lett.*, vol. 16, pp. 665–668, 2017.
[21] Q.-X. Chu, D.-L. Wen, and Y. Luo, "A broadband ±45° dual-polarized antenna with Y-Shaped feeding lines," *IEEE Trans. Antennas Propag.*, vol. 63, no. 2, pp. 483–490, Feb. 2015.
[22] D.-Z. Zheng and Q.-X. Chu, "A multimode wideband ±45° dual-polarized antenna with embedded loops," *IEEE Antennas Wireless Propag. Lett.*, vol. 17, pp. 633–636, 2017.
[23] R. Wu and Q.-X. Chu, "A broadband dual-polarized antenna with chamfers," *Microw. Opt. Technol. Lett.*, vol. 59, no. 3, pp. 631–635, Mar. 2017.
[24] D.-Z. Zheng and Q.-X. Chu, "A wideband dual-polarized antenna with two independently controllable resonant modes and its array for base-station applications," *IEEE Antennas Wireless Propag. Lett.*, vol. 16, pp. 2014–2017, 2017.
[25] Q. Zhang and Y. Gao, "A compact broadband dual-polarized antenna array for base stations," *IEEE Antennas Wireless Propag. Lett.*, vol. 17, no. 6, pp. 1073–1076, Jun. 2018.
[26] H. Huang, Y. Liu, and S. Gong, "A novel dual-broadband and dual-polarized antenna for 2G/3G/LTE base stations," *IEEE Trans. Antennas Propag.*, vol. 64, no. 9, pp. 4113–4118, Sep. 2016.
[27] Y. He, J. Li, S. W. Wong, X. Pan, L. Zhang, and Z. N. Chen, "A miniaturized base station antenna with novel phase shifter for 3G/LTE applications," *IEEE Access*, vol. 6, pp. 52877–52888, 2018.
[28] Y. Cui, R. Li, and P. Wang, "Novel dual-broadband planar antenna and its array for 2G/3G/LTE base stations," *IEEE Trans. Antennas Propag.*, vol. 61, no. 3, pp. 1132–1139, Mar. 2013.
[29] R. Wu and Q.-X. Chu, "A compact, dual-polarized multiband array for 2G/3G/4G base stations," *IEEE Trans. Antennas Propag.*, vol. 67, no. 4, pp. 2298–2304, Apr. 2019.
[30] X. W. Dai, Z. Y. Wang, X. C. Gao, G. Q. Luo, and Z. C. Hao, "Compact dual-broadband dual-polarized antenna with additional ground platform," *IEEE Access*, vol. 7, pp. 50650–50657, 2019.
[31] Y. Zhang, X. Y. Zhang, L.-H. Ye, and Y.-M. Pan, "Dual-band base station array using filtering antenna elements for mutual coupling suppression," *IEEE Trans. Antennas Propag.*, vol. 64, no. 8, pp. 3423–3430, Aug. 2016.
[32] Q.-X. Chu, D.-L. Wen, and Y. Luo, "Principle of multimode broadband antennas with resonator-loaded dipole," in *Proc. Int. Workshop Antenna Technol. (iWAT)*, Seoul, South Korea, Mar. 2015, pp. 45–47.
[33] F. Hyjazie, P. Watson, and H. Boutayeb, "Dual band interleaved base station phased array antenna with optimized cross-dipole and EBG/AMC structure," in *Proc. IEEE Antennas Propag. Soc. Int. Symp. (APSURSI)*, Jul. 2014, pp. 1558–1559.
[34] *Commscope Corp*. Accessed: Apr. 2, 2020. [Online]. Available: https://www.commscope.com/product-type/antennas/base-station-antennas-equipment/base-station-antennas
[35] C. A. Balanis, *Antenna Theory: Analysis and Design*, 4th ed. Hoboken, NJ, USA: Wiley, 2016.

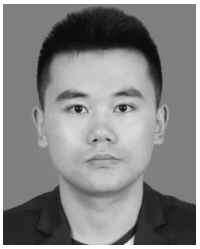

DONGZE ZHENG (Student Member, IEEE) was born in Bozhou, Anhui, China, in 1993. He received the B.S. degree from Anhui University, Hefei, China, in 2014, and the M.E. degree from the South China University of Technology (SCUT), Guangzhou, China, in 2017. He is currently pursuing the Ph.D. degree with the Polytechnique Montréal (University of Montreal), QC, Canada. His master's thesis was one of the excellent theses in SCUT. He has authored/coauthored several academic journal articles and conference papers. His current research interests include periodic structures, transmission lines, leaky-wave antennas, wideband antennas, base-station antennas, circularly polarized antennas, filters, and FMCW systems. He was the Outstanding Graduate in Anhui Province. He serves as a Reviewer for several international journals, such as the IEEE TRANSACTIONS ON ANTENNAS AND PROPAGATION, the IEEE ANTENNAS AND WIRELESS PROPAGATION LETTERS, and IEEE ACCESS.

YU LUO (Member, IEEE) received the B.S. and Ph.D. degrees in electronic engineering from the South China University of Technology, Guangzhou, Guangdong, China, in 2010 and 2015, respectively. He worked as a Research Assistant with the University of Macau, Macau, from April 2014 to September 2014. He worked as a Postdoctoral Fellow with the University of Victoria, BC, Canada, from September 2015 to August 2016. He was a Research Fellow with the National University of Singapore, from September 2016 to September 2018. He is currently a Professor with the School of Microelectronics, Tianjin University. He has authored or coauthored more than 30 technical articles. His research interests include antennas in new generation mobile communications systems, such as SIW antennas, base-station antennas, circularly polarized antennas, MIO antennas, Yagi-Uda antennas, and mmW/THz antennas. He is a Senior Member of China Electronic Institute (CEI).

QING-XIN CHU (Fellow, IEEE) received the B.S., M.E., and Ph.D. degrees in electronic engineering from Xidian University, Xi'an, Shaanxi, China, in 1982, 1987, and 1994, respectively. He was with the School of Electronic Engineering, Xidian University, from January 1982 to January 2004, where he was also a Professor and the Vice Dean of the School of Electronic Engineering, from December 1997 to January 2004. He is currently a Professor with the School of Electronic and Information Engineering, and the Director of the Research Institute of Antennas and RF Techniques and the Engineering Center of Antennas and RF Techniques of Guangdong Province, South China University of Technology. He is the Founder and the Chair of IEEE Guangzhou AP/MTT Chapter, the Vice-Chair of China Electronic Institute (CEI) Antenna Society, and the CEI Fellow. He has published over 400 articles in journals and conferences with over 3000 SCI citations, in which several articles published in the IEEE TRANSACTIONS ON ANTENNAS AND PROPAGATION OR MICROWAVE THEORY AND TECHNIQUES became the top ESI (Essential Science Indicators) articles, since 2008. His current research interests include antennas and microwave devices in wireless communication. He was elected as the highly cited scholar by Elsevier in the field of Electrical and Electronic Engineering, in 2013. He has authorized more than 60 invention patents of China. He was a recipient of the Science Awards by CEI, in 2018 and 2016, the Science Award by Guangdong Province of China, in 2013, the Science Awards by the Education Ministry of China, in 2008 and 2002, the Fellowship Award by Japan Society for Promotion of Science (JSPS), in 2004, the Singapore Tan Chin Tuan Exchange Fellowship Award, in 2003, the Educational Award by Shaanxi Province, in 2003. He is currently an Associate Editor of *Radio Science* and *IET Electronic Letters*.